PLASTICITÉ CRISTALLINE ET TRANSITION D'ÉCHELLE : CAS DU MONOCRISTAL

—

12/12/2016

Lionel MARCIN (Safran Tech/M&P), *lionel.marcin@safrangroup.com*

SAFRAN

Outline

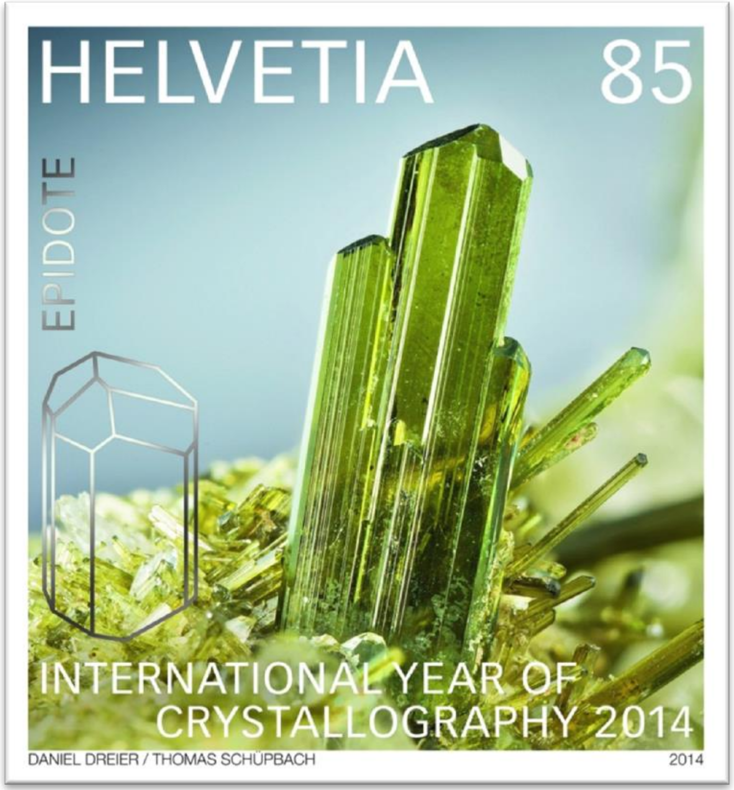

1. Introduction & motivation

2. Physical origins of crystal slip

Experimental observations

Taylor’s paradox

Dislocations

3. Continuum crystal plasticity

The schmid law

Geometry of slip and Schmid factors in FCC crystals

Constitutive rules for single crystal plasticity

Example of monocrystal behaviour

Example of FE computation

Outline

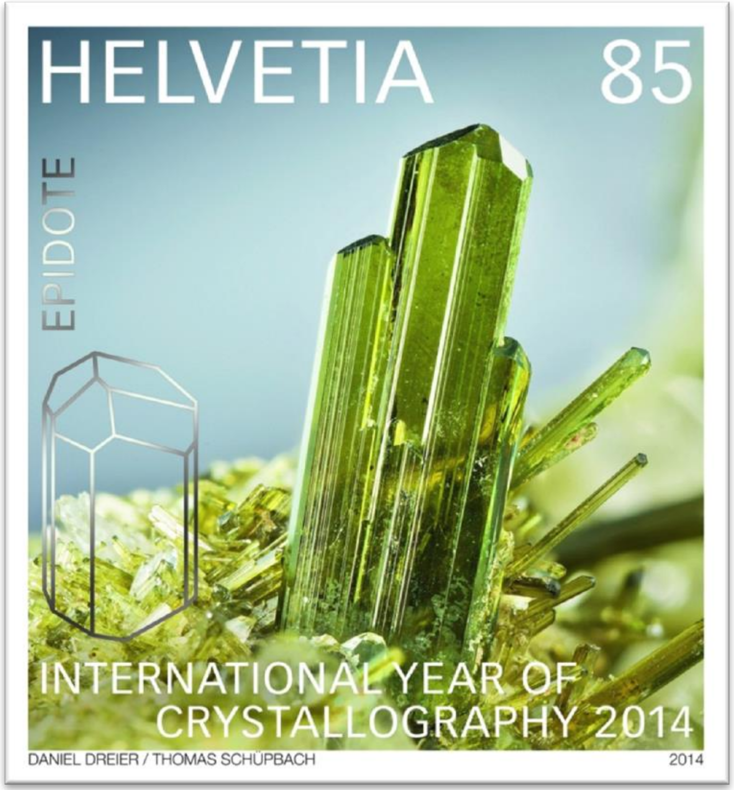

1. Introduction & motivation

2. Physical origins of crystal slip

Experimental observations

Taylor's paradox

Dislocations

3. Continuum crystal plasticity

The schmid law

Geometry of slip and Schmid factors in FCC crystals

Constitutive rules for single crystal plasticity

Example of monocrystal behaviour

Example of FE computation

Deformation of crystalline materials : a multiscale problem

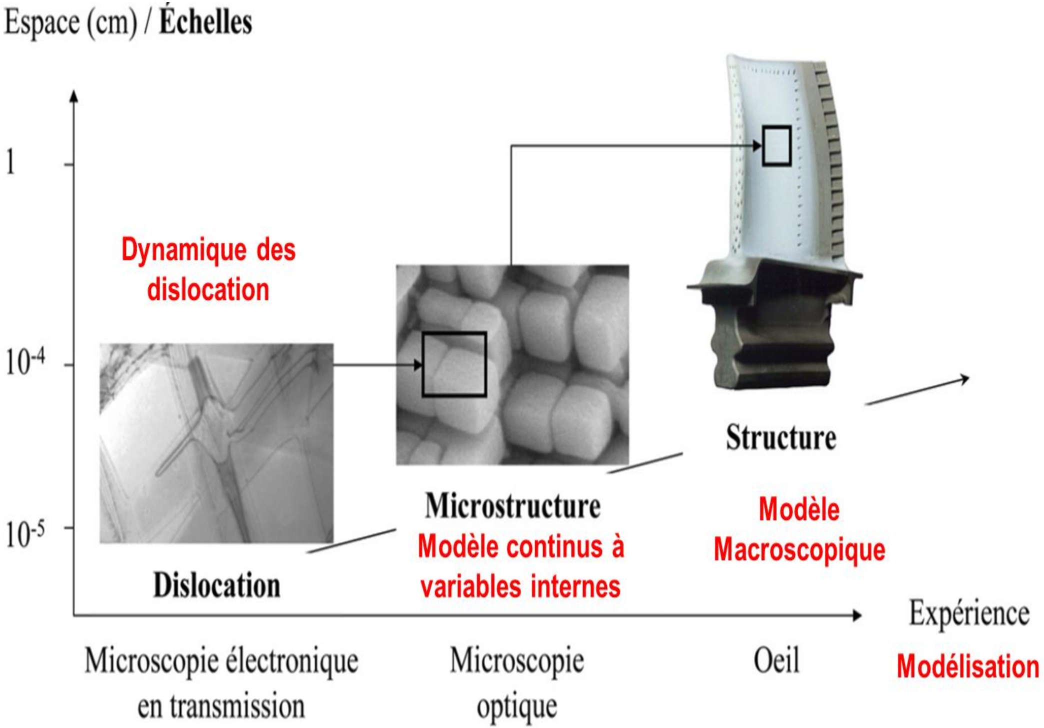

Plastic deformation results in the motion of lots of defects in the crystal lattice (dislocations)
→ continuum scale (> µm)

Integrated Computational Materials Engineering

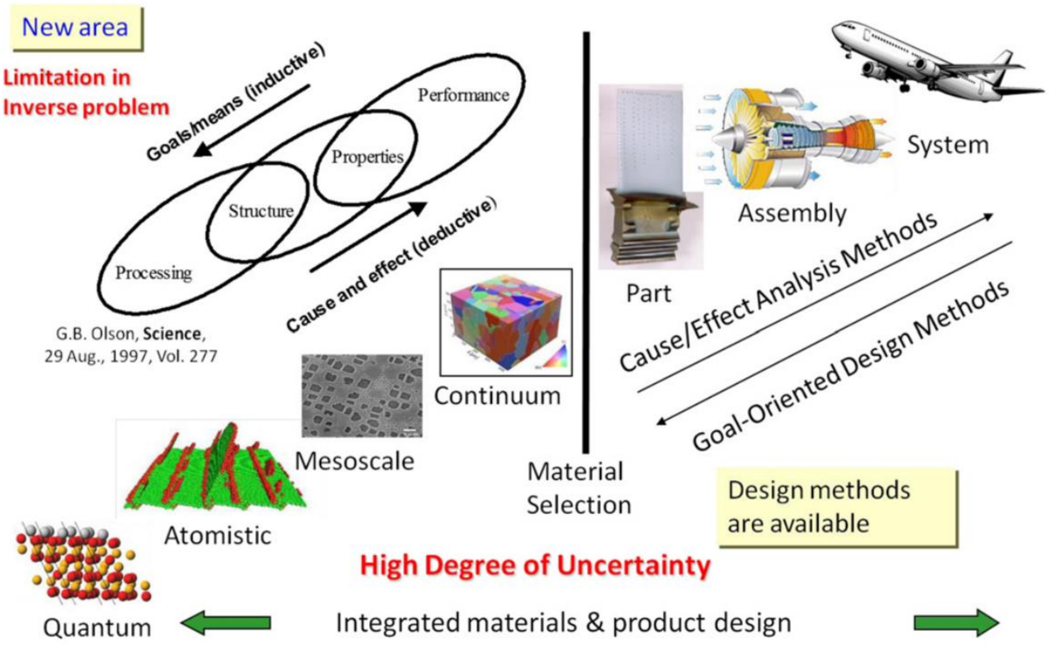

Local values (as opposed to mean values) are crucial when studying deformation and fracture → model for crystal plasticity needed.

Such applications in aeronautic (Safran sources)

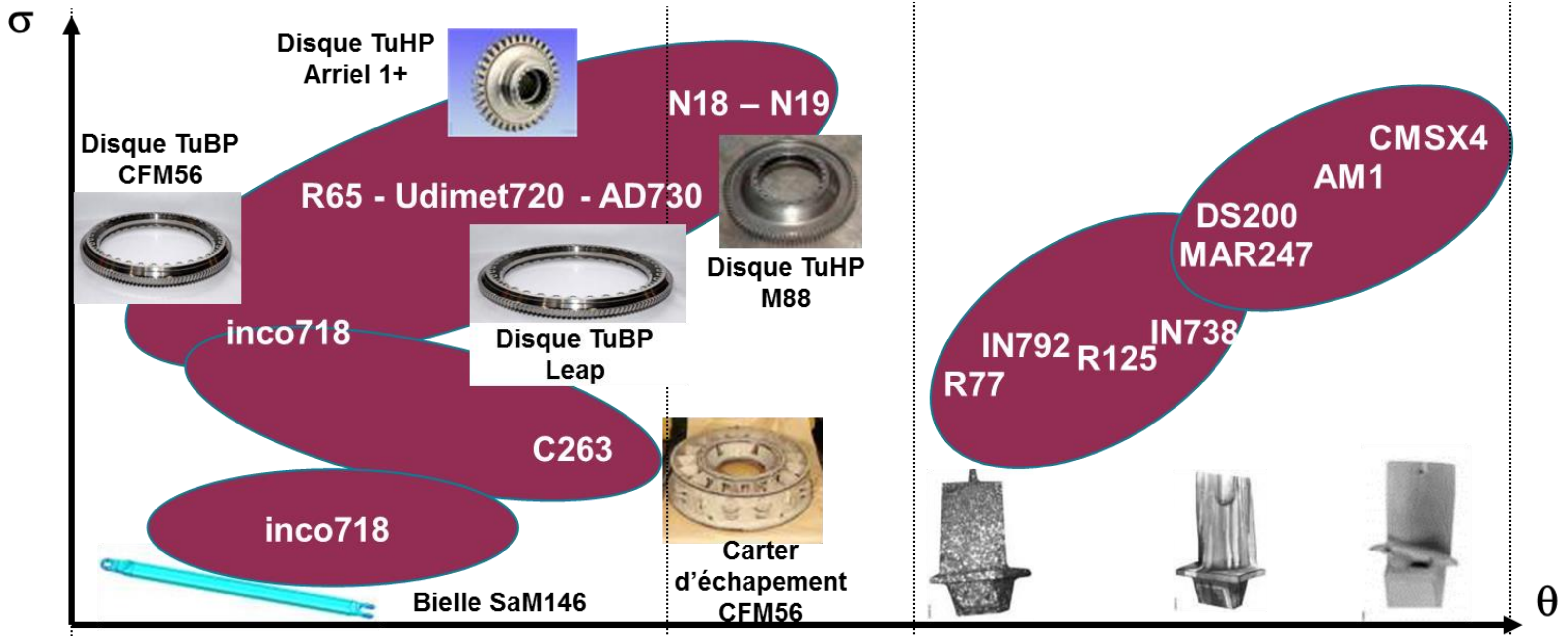

Forgeage conventionnel Laminage fluotournage	Forgeage Isotherme	équiaxe	dirigée	monocristal
		Fonderie		

Such applications in electronics (Single crystal)

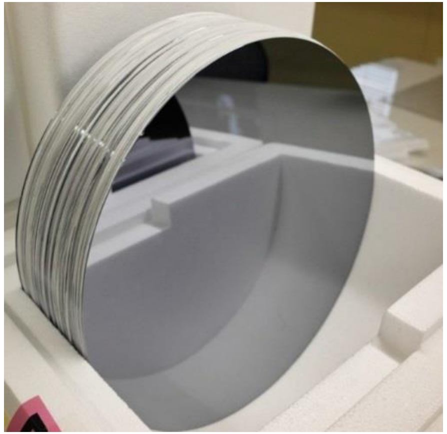

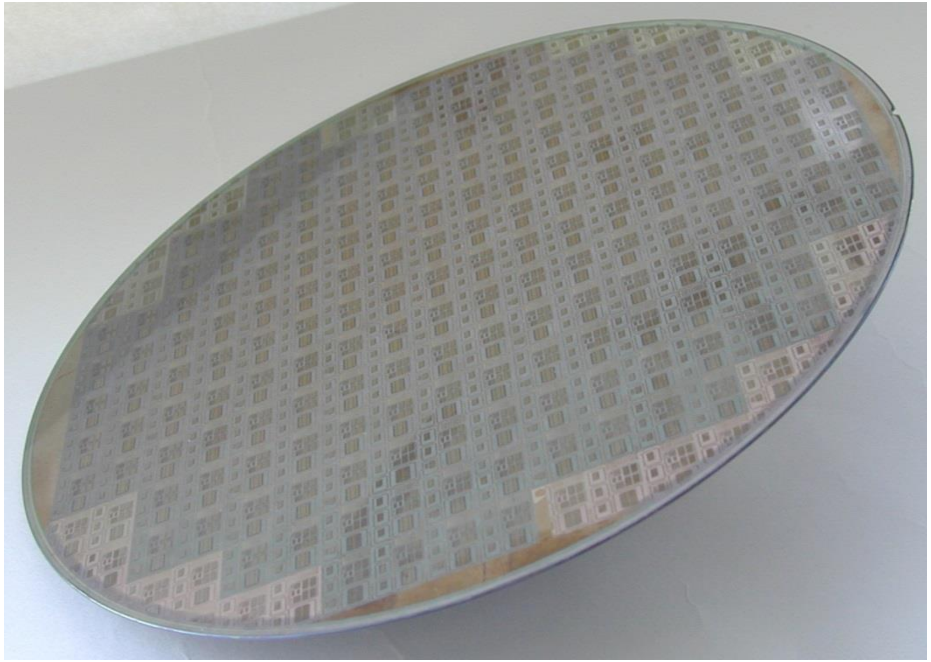

Outline

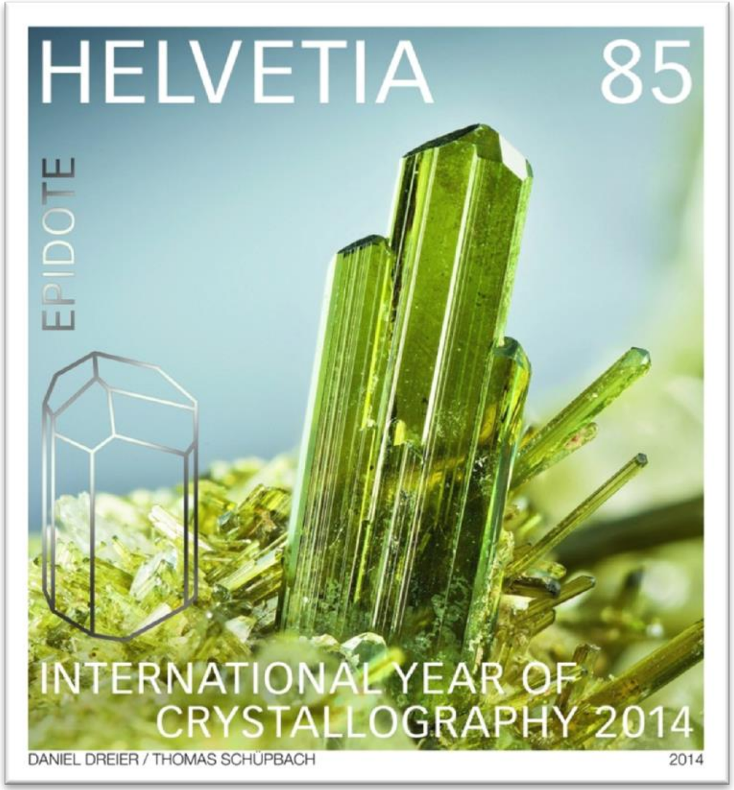

1. Introduction & motivation

2. Physical origins of crystal slip

Experimental observations

Taylor's paradox

Dislocations

3. Continuum crystal plasticity

The schmid law

Geometry of slip and Schmid factors in FCC crystals

Constitutive rules for single crystal plasticity

Example of monocrystal behaviour

Example of FE computation

A brief history

V.Volterra

1860 - 1940

G.I.Taylor

1886 - 1975

M.Polanyi

1891 - 1976

E.Orowan

1891 - 1976

P.B.Hirsch

1920 -

The early of the history of dislocation theory. 1907: Definition of Volterra’s dislocation (or isolated defect) by the mathematician V. Volterra; 1934: Discovery of the concept of crystal dislocation introduced by Orowan, Polany and Taylor; 1956: First published observations of dislocations by transmission electron microscopy.

60 years of plastic slip in monocrystals

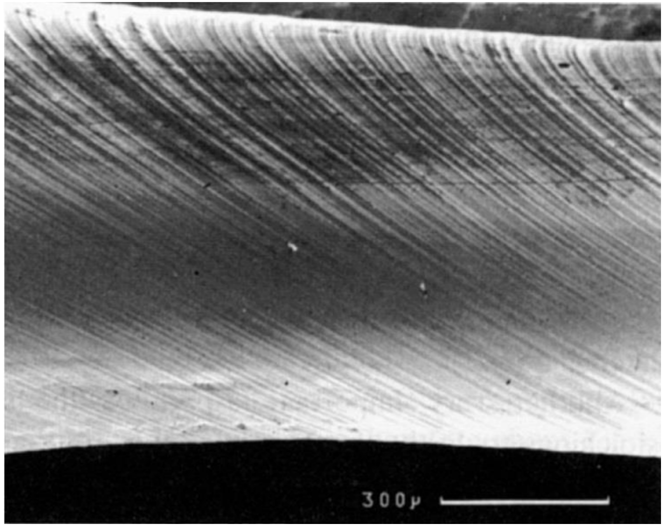

Cadmium monocrystal deformed under tension [Schmid and Boas, 1950]

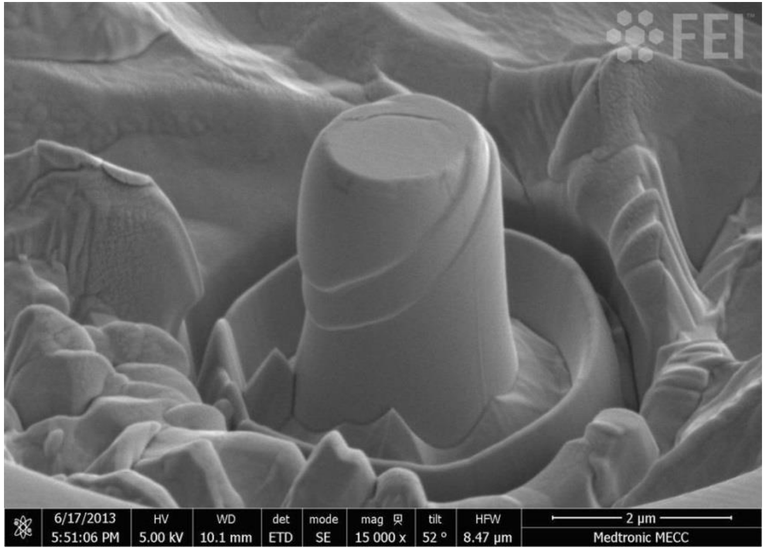

Fib fabricated micropillar deformed under compression [Shan et al., 2007]

Conclusion : Crystals deform by shear. Shear appear to be localized on the highest atomic density planes, the so-called *slip planes*.

Evidences of crystallographic slip in Ni-based superalloy

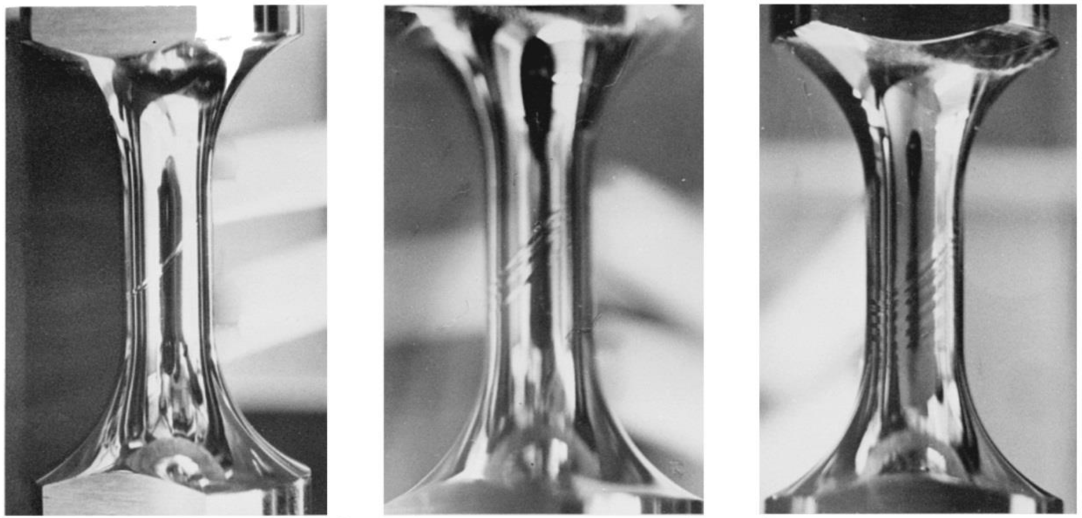

5 mm 5 mm

N = 3/4 de cycle N = 2 cycles N = 11 cycles

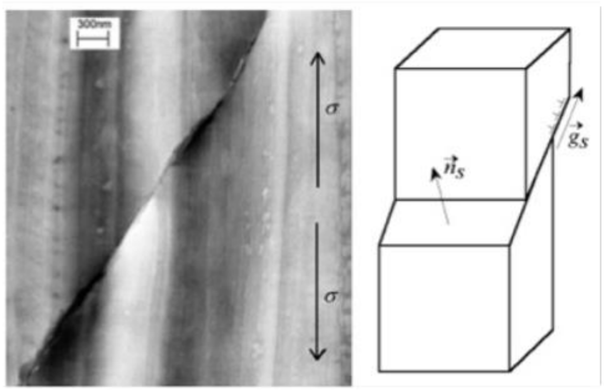

With each passage of a dislocation through a single crystal corresponds the appearance of a "walk" on the surface and a shift of the two parts. The set of these shifts generates the plastic deformation observable on the macroscopic scale

The concept of dislocation (1/2)

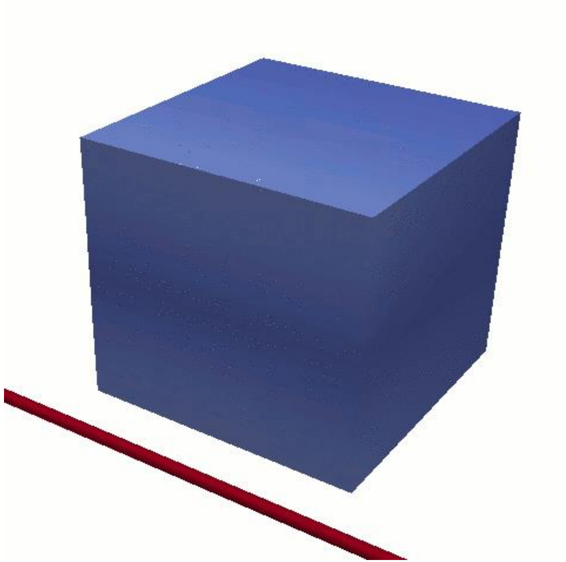

pure edge

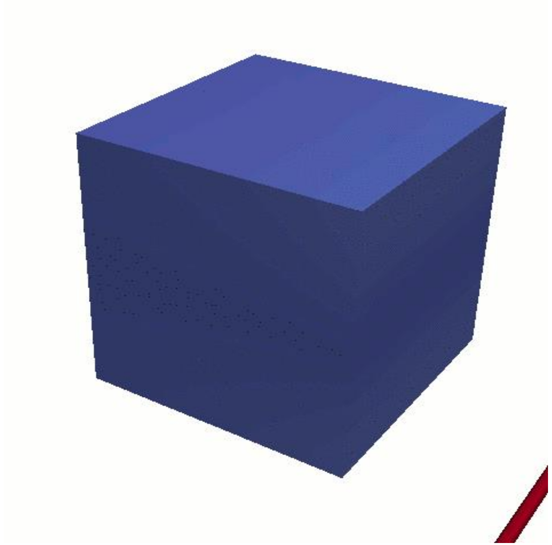

pure screw

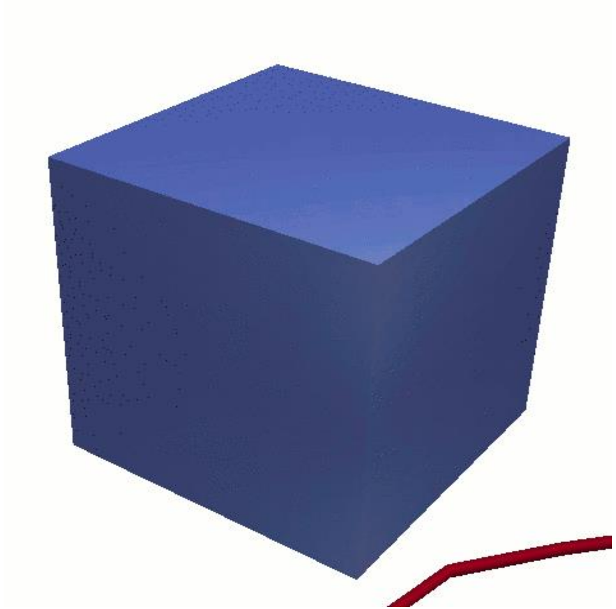

mixed dislocation

The concept of dislocation (2/2)

A dislocation can be represented by :

- a line vector ***L***
- a Bürgers vector ***b***

Dislocations may pre-exist and are created during plastic deformation.

- The sum of the Burgers vector of created dislocations is equal to zero

A dislocation moves

- The motion is defined by a glide plane (*L* , *b*) and a glide direction *g*
- Screw dislocation don’t have a single glide plane
- Edge dislocation do have a single glide plane
- Plastic deformation is associated to the flux of disloc

The crystal is distorted around dislocation

- Dislocations are stress concentrators
- There is an elastic energy associated to dislocations

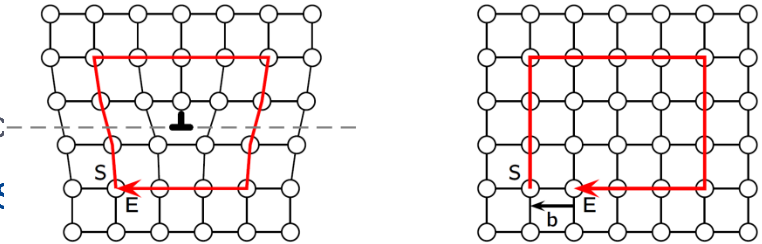

dislocated network   perfect network

SAFRAN

Can we actually see dislocations ?

Microscope FEI TECNAI F20-ST
Centre des Matériaux – MINES ParisTech

Bright field image
Dislocation microstructure of deformed Ti-6242 alloy

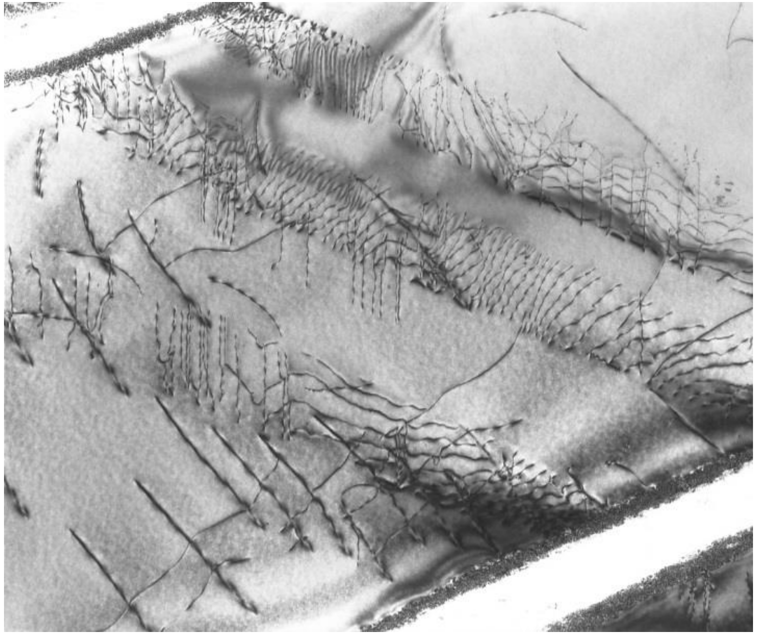

Can we actually see dislocations ?

Bright field image
Dislocation microstructure of deformed Ti-6242 alloy

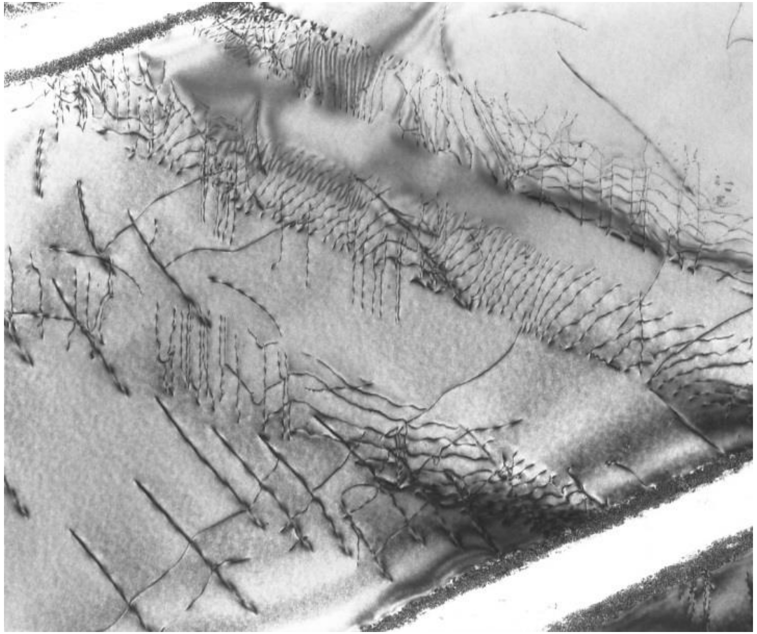

In 1cm3 of metal alloys (order of magnitude):

- **10m of dislocation in a single crystal alloy**
- **10.000km in a polycrystal weakly hardened**
- **10.000.000km in a highly hardened polycrystal**

Outline

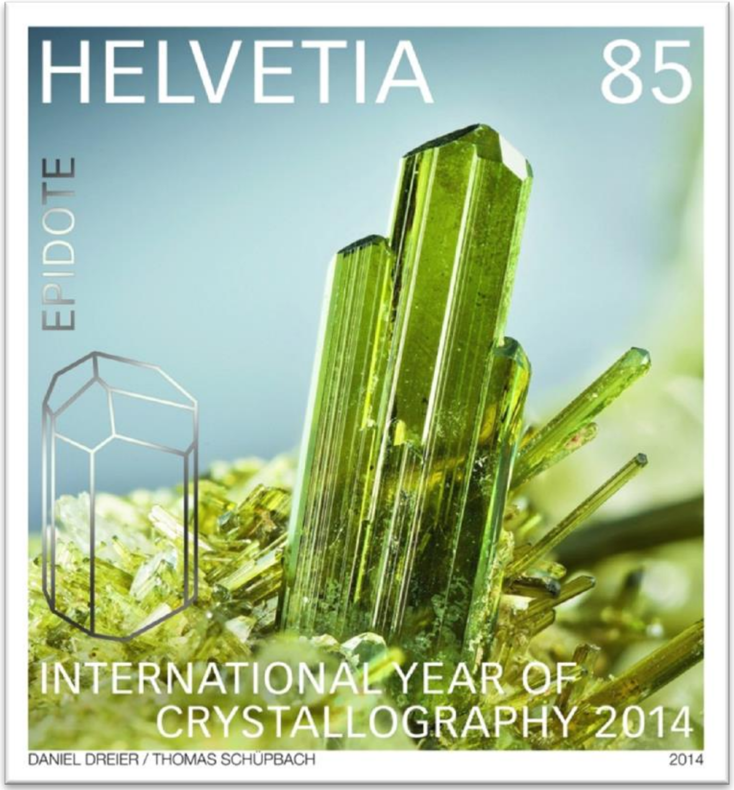

1. Introduction & motivation

2. Physical origins of crystal slip

Experimental observations

Taylor’s paradox

Dislocations

3. Continuum crystal plasticity

The schmid law

Geometry of slip and Schmid factors in FCC crystals

Constitutive rules for single crystal plasticity

Example of monocrystal behaviour

Example of FE computation

Tensile test apllied to SX - *Resolved shear stress*

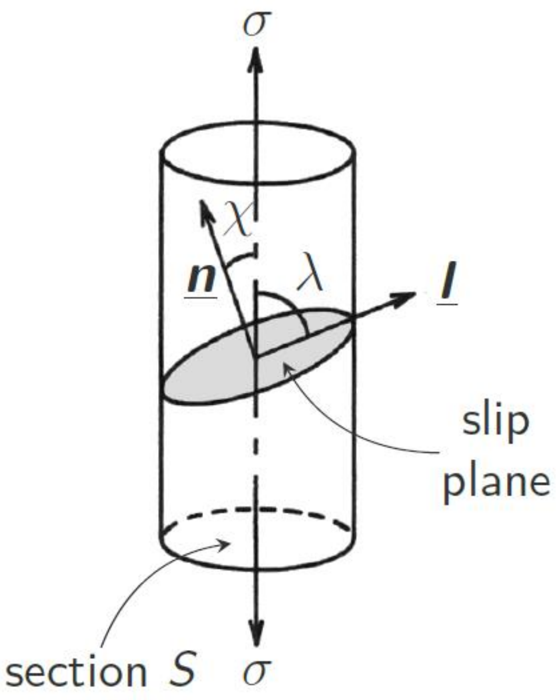

Given a slip direction ***l*** contained in a slip plane with a normal vector ***n*** , the shear τ in the slip direction can be related to the applied tensile stress σ :

$$\tau = \frac{F\cos(\lambda)}{S/\cos(\chi)} = \sigma\cos(\lambda)\cos(\chi)$$

m = cos(λ) cos(χ) 2 [0, 0.5] is called the **Schmid factor**.

Generalization, in tensorial form we have :

$$\tau = l_i \sigma_{ij} n_j$$

The critical resolved shear stress

Experiments of Schmid and Boas

- No influence of the normal stress operating on the glide plane.
- *A critical value of the resolved shear stress is required for the initiation of glide*.

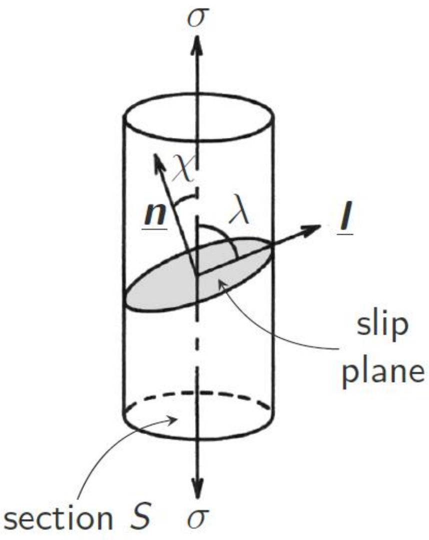

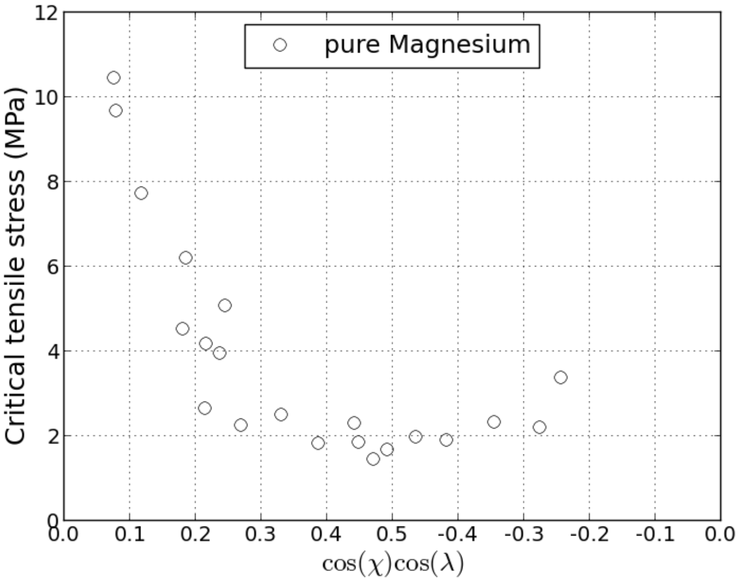

The critical resolved shear stress

Experiments of Schmid and Boas

- No influence of the normal stress operating on the glide plane.
- *A critical value of the resolved shear stress is required for the initiation of glide*.

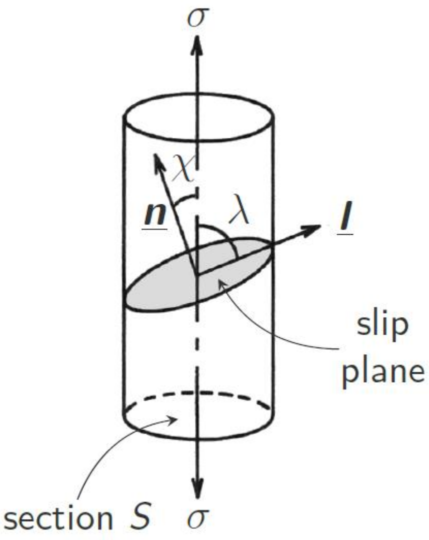

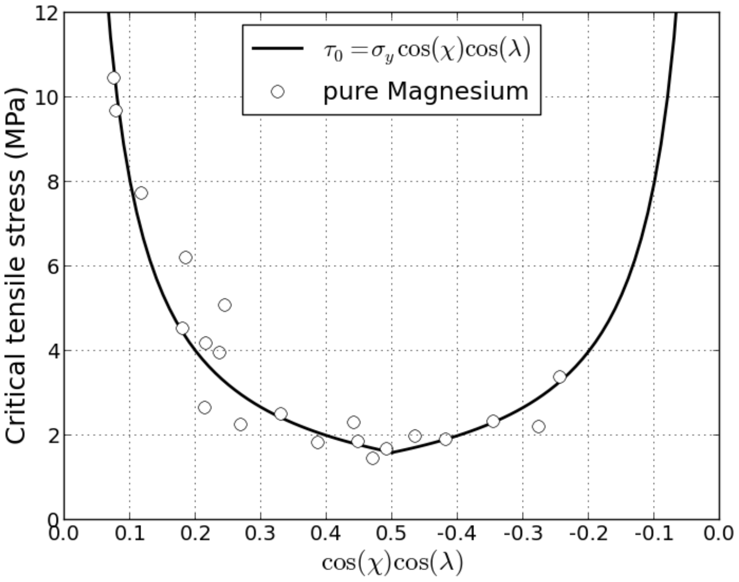

The critical resolved shear stress

More experimental data on critical resolved shear stress:

Mg data from [Schmid1950]

Zn data from [Jillson]

Cd data from [Andrade & Roscoe]

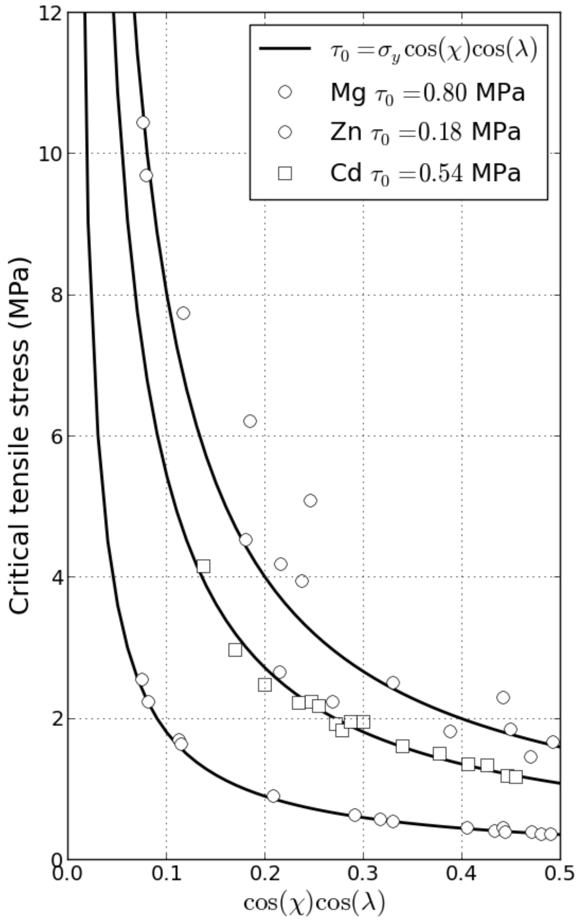

Some important crystalline structures

Face centered cubic

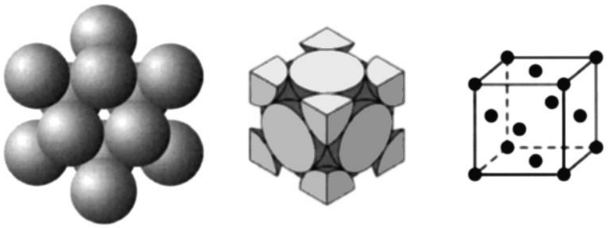

Body centered cubic

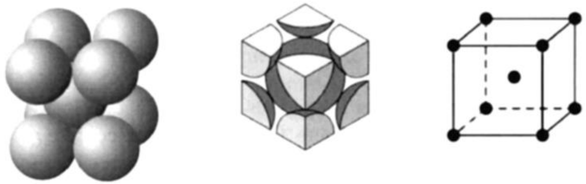

Hexagonal close packing

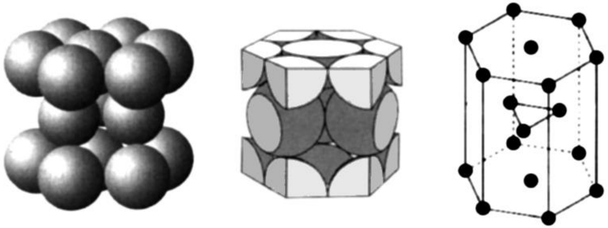

Slip systems in FCC crystals

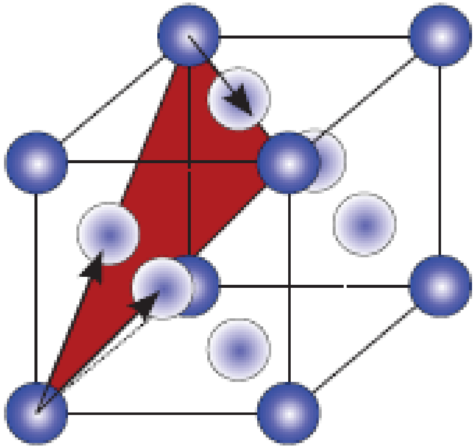

Octaedral slip

4 slip planes {111} i.e. (111), (111), (111), (111) indicated by normals

3 slip directions of type <110> in each 111 plane

number	1	2	3	4	5	6
name	B4	B2	B5	D4	D1	D6
plane	(111)	(111)	(111)	$(1\bar{1}1)$	$(1\bar{1}1)$	$(1\bar{1}1)$
direction	$[\bar{1}01]$	$[0\bar{1}1]$	$[\bar{1}10]$	$[\bar{1}01]$	[011]	[110]

number	7	8	9	10	11	12
name	A2	A6	A3	C5	C3	C1
plane	$(\bar{1}11)$	$(\bar{1}11)$	$(\bar{1}11)$	$(11\bar{1})$	$(11\bar{1})$	$(11\bar{1})$
direction	$[0\bar{1}1]$	[110]	[101]	$[\bar{1}10]$	[101]	[011]

Simple tension for a single crystal specimen

Tensile test in the direction [001]

Schmid factor $m^s = (\boldsymbol{n}^s . \boldsymbol{t})\,(\boldsymbol{l}^s . \boldsymbol{t})$

number	1	2	3	4	5	6
name	B4	B2	B5	D4	D1	D6
plane	(111)	(111)	(111)	$(1\bar{1}1)$	$(1\bar{1}1)$	$(1\bar{1}1)$
direction	$[\bar{1}01]$	$[0\bar{1}1]$	$[\bar{1}10]$	$[\bar{1}01]$	$[011]$	$[110]$
Schmid factor						

number	7	8	9	10	11	12
name	A2	A6	A3	C5	C3	C1
plane	$(\bar{1}11)$	$(\bar{1}11)$	$(\bar{1}11)$	$(11\bar{1})$	$(11\bar{1})$	$(11\bar{1})$
direction	$[0\bar{1}1]$	$[110]$	$[101]$	$[\bar{1}10]$	$[101]$	$[011]$
Schmid factor						

Simple tension for a single crystal specimen

Tensile test in the direction [001]

8 active slip systems

Schmid factor $m^s = (\boldsymbol{n}^s . \boldsymbol{t})\,(\boldsymbol{l}^s . \boldsymbol{t})$

number	1	2	3	4	5	6
name	B4	B2	B5	D4	D1	D6
plane	(111)	(111)	(111)	$(1\bar{1}1)$	$(1\bar{1}1)$	$(1\bar{1}1)$
direction	$[\bar{1}01]$	$[0\bar{1}1]$	$[\bar{1}10]$	$[\bar{1}01]$	$[011]$	$[110]$
Schmid factor	$\frac{1}{\sqrt{6}}$	$\frac{1}{\sqrt{6}}$	0	$\frac{1}{\sqrt{6}}$	$\frac{1}{\sqrt{6}}$	0

number	7	8	9	10	11	12
name	A2	A6	A3	C5	C3	C1
plane	$(\bar{1}11)$	$(\bar{1}11)$	$(\bar{1}11)$	$(11\bar{1})$	$(11\bar{1})$	$(11\bar{1})$
direction	$[0\bar{1}1]$	$[110]$	$[101]$	$[\bar{1}10]$	$[101]$	$[011]$
Schmid factor	$\frac{1}{\sqrt{6}}$	0	$\frac{1}{\sqrt{6}}$	0	$-\frac{1}{\sqrt{6}}$	$-\frac{1}{\sqrt{6}}$

Simple tension for a single crystal specimen

Tensile test in the direction [111]

Schmid factor $m^s = (\boldsymbol{n}^s . \boldsymbol{t})\ (\boldsymbol{l}^s . \boldsymbol{t})$

number	1	2	3	4	5	6
name	B4	B2	B5	D4	D1	D6
plane	(111)	(111)	(111)	$(1\bar{1}1)$	$(1\bar{1}1)$	$(1\bar{1}1)$
direction	$[\bar{1}01]$	$[0\bar{1}1]$	$[\bar{1}10]$	$[\bar{1}01]$	$[011]$	$[110]$
Schmid factor						

number	7	8	9	10	11	12
name	A2	A6	A3	C5	C3	C1
plane	$(\bar{1}11)$	$(\bar{1}11)$	$(\bar{1}11)$	$(11\bar{1})$	$(11\bar{1})$	$(11\bar{1})$
direction	$[0\bar{1}1]$	$[110]$	$[101]$	$[\bar{1}10]$	$[101]$	$[011]$
Schmid factor						

Simple tension for a single crystal specimen

Tensile test in the direction [111]

6 active slip systems

Schmid factor $m^s = (\boldsymbol{n}^s . \boldsymbol{t})(\boldsymbol{l}^s . \boldsymbol{t})$

number	1	2	3	4	5	6
name	B4	B2	B5	D4	D1	D6
plane	(111)	(111)	(111)	$(1\bar{1}1)$	$(1\bar{1}1)$	$(1\bar{1}1)$
direction	$[\bar{1}01]$	$[0\bar{1}1]$	$[\bar{1}10]$	$[\bar{1}01]$	$[011]$	$[110]$
Schmid factor	0	0	0	0	$\frac{2}{3\sqrt{6}}$	$\frac{2}{3\sqrt{6}}$

number	7	8	9	10	11	12
name	A2	A6	A3	C5	C3	C1
plane	$(\bar{1}11)$	$(\bar{1}11)$	$(\bar{1}11)$	$(11\bar{1})$	$(11\bar{1})$	$(11\bar{1})$
direction	$[0\bar{1}1]$	$[110]$	$[101]$	$[\bar{1}10]$	$[101]$	$[011]$
Schmid factor	0	$\frac{2}{3\sqrt{6}}$	$\frac{2}{3\sqrt{6}}$	0	$\frac{2}{3\sqrt{6}}$	$\frac{2}{3\sqrt{6}}$

Simple tension for a single crystal specimen

Tensile test in the direction [011]

Schmid factor $m^s = (\boldsymbol{n}^s . \boldsymbol{t})\, (\boldsymbol{l}^s . \boldsymbol{t})$

number	1	2	3	4	5	6
name	B4	B2	B5	D4	D1	D6
plane	(111)	(111)	(111)	$(1\bar{1}1)$	$(1\bar{1}1)$	$(1\bar{1}1)$
direction	$[\bar{1}01]$	$[0\bar{1}1]$	$[\bar{1}10]$	$[\bar{1}01]$	$[011]$	$[110]$
Schmid factor						

number	7	8	9	10	11	12
name	A2	A6	A3	C5	C3	C1
plane	$(\bar{1}11)$	$(\bar{1}11)$	$(\bar{1}11)$	$(11\bar{1})$	$(11\bar{1})$	$(11\bar{1})$
direction	$[0\bar{1}1]$	$[110]$	$[101]$	$[\bar{1}10]$	$[101]$	$[011]$
Schmid factor						

Simple tension for a single crystal specimen

Tensile test in the direction [011]

4 active slip systems

Schmid factor $m^s = (\boldsymbol{n}^s . \boldsymbol{t})(\boldsymbol{l}^s . \boldsymbol{t})$

number	1	2	3	4	5	6
name	B4	B2	B5	D4	D1	D6
plane	(111)	(111)	(111)	$(1\bar{1}1)$	$(1\bar{1}1)$	$(1\bar{1}1)$
direction	$[\bar{1}01]$	$[0\bar{1}1]$	$[\bar{1}10]$	$[\bar{1}01]$	$[011]$	$[110]$
Schmid factor	$\frac{1}{\sqrt{3}}$	0	$\frac{1}{\sqrt{3}}$	0	0	0

number	7	8	9	10	11	12
name	A2	A6	A3	C5	C3	C1
plane	$(\bar{1}11)$	$(\bar{1}11)$	$(\bar{1}11)$	$(11\bar{1})$	$(11\bar{1})$	$(11\bar{1})$
direction	$[0\bar{1}1]$	$[110]$	$[101]$	$[\bar{1}10]$	$[101]$	$[011]$
Schmid factor	0	$\frac{1}{\sqrt{3}}$	$\frac{1}{\sqrt{3}}$	0	0	0

Summary: inverse pole figure

First activated slip systems in tension according to Schmid law:

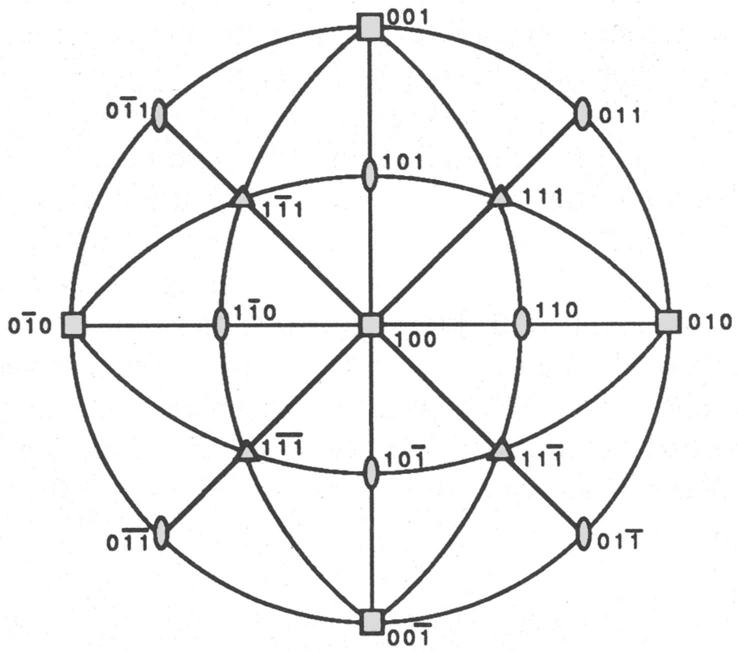

[001] tension

[111] tension

[110] tension

Summary: inverse pole figure

First activated slip systems in tension according to Schmid law:

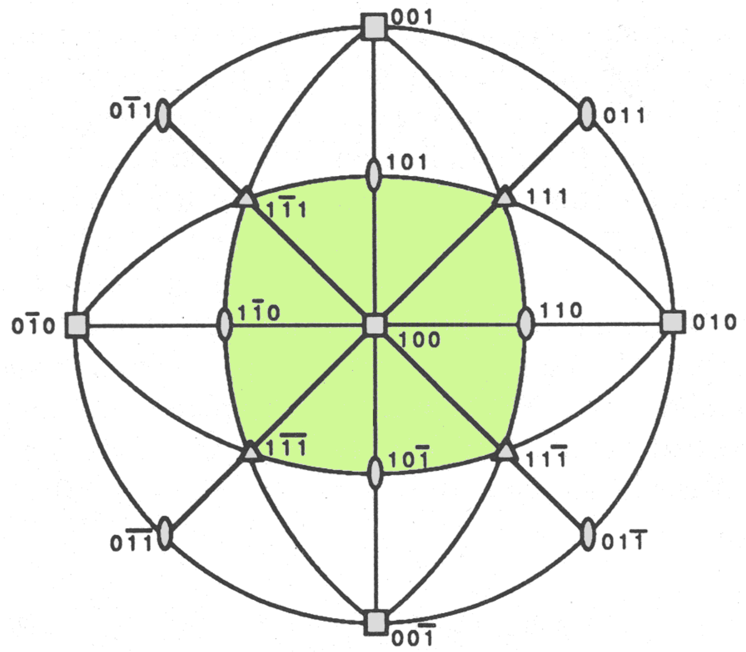

[001] tension

8 slip systems :
B4, C1, A2, D4,
C3, B2, D1, A3

[111] tension

[110] tension

Summary: inverse pole figure

First activated slip systems in tension according to Schmid law:

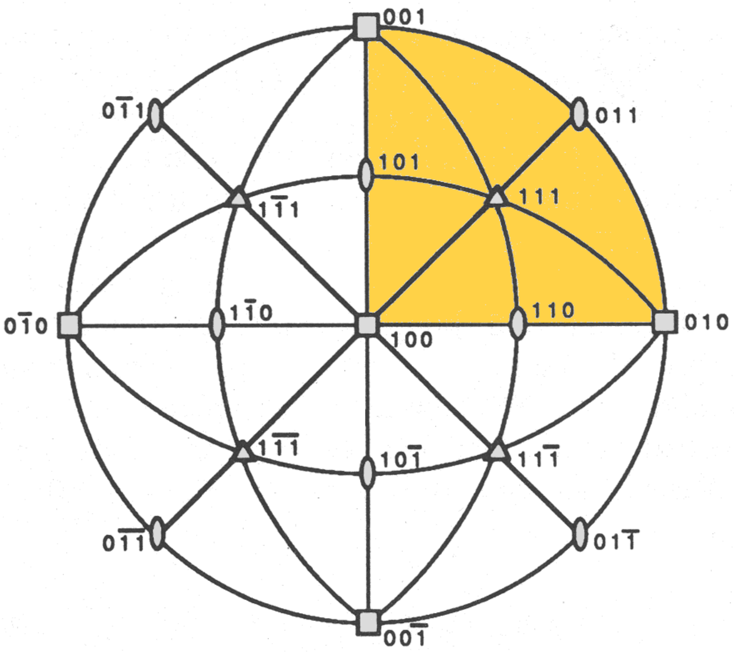

[001] tension

8 slip systems :
B4, C1, A2, D4,
C3, B2, D1, A3

[111] tension

6 slip systems :
D4, D1, C1, C5,
B4, B5

[110] tension

Summary: inverse pole figure

First activated slip systems in tension according to Schmid law:

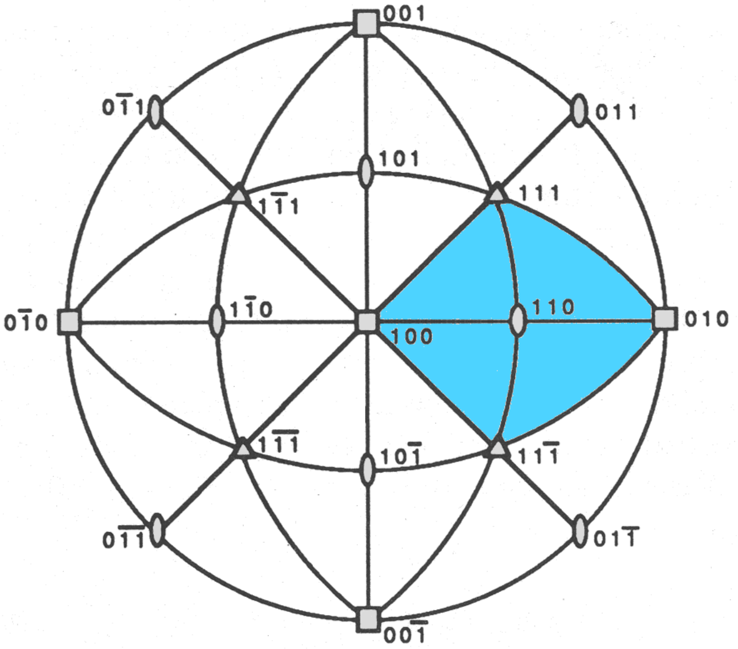

[001] tension
8 slip systems :
B4, C1, A2, D4, C3, B2, D1, A3

[111] tension
6 slip systems :
D4, D1, C1, C5, B4, B5

[110] tension
4 slip systems :
B4, A3, B5, A6

Historical developments of the theory

- The initial foundations are laid out by the pioneering work of **Taylor** in 1938 [Taylor, 1938].
- The theory was since further developed by **Bishop & Hill** [Bishop and Hill, 1951], **Kocks** [Kocks and Brown, 1966, Kocks, 1970], **Hill and Rice** [Hill, 1966, Hill and Rice, 1972], **Asaro and Rice** [Asaro, 1975, Asaro and Rice, 1977], **Havner** [Havner, 1992], **Cailletaud** [Meric et al., 1991, Meric and Cailletaud, 1991].

Rate sensitive plastic slip

The Schmid law predicting an elastic-perfectly plastic behaviour cannot describe typical () curves. The plastic slip on a given slip system *s* (***ns*** , ***ls***) is rate sensitive and can be described by a power law.

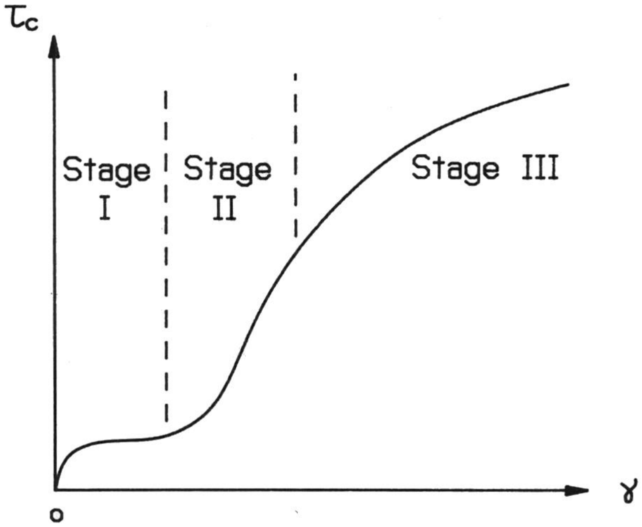

Two main formulations exist in the literature :

Multiplicative

$$\dot{\gamma}^s = \dot{\gamma}_0 (\frac{\tau^s}{\tau_0})^n sign(\tau^s)$$

Additive with threshold

$$\dot{\gamma}^s = \left\langle \frac{\left|\tau^s\right| - \tau_0}{K} \right\rangle sign(\tau^s)$$

τ_0 is the critical resolved shear stress, $\dot{\gamma}_0$, *K* and *n* are parameters.

Basic ingredients of crystal plasticity

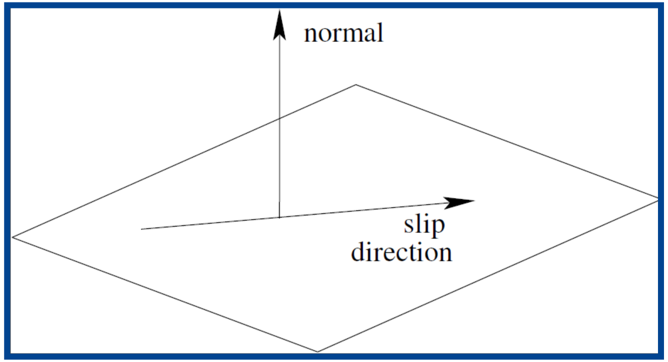

A collection of *N* slip systems

Normal to slip plane ***n^s***

Direction of slip system ***l^s***

Orientation tensor $\underset{=}{m}^s = \frac{1}{2}(\vec{n}^s \otimes \vec{l}^s + \vec{l}^s \otimes \vec{n}^s)$

Resolved shear stress $\tau^s = \underline{\sigma} : \underline{m}^s = \underline{\sigma} : \frac{1}{2}(\vec{l}^s \otimes \vec{n}^s + \vec{n}^s \otimes \vec{l}^s)$

Yield function $f^s(\tau^s, \text{hardening variables}, \ldots) = 0$

Elastic behavior $\forall s,\ f^s < 0$

Shear strain rate $\dot{\gamma}^s = \dot{\gamma}^s(f^s)$

Small strain formalism and schmid law

- Strain partition into elastic and plastic parts

$$\underline{\varepsilon} = \underline{\varepsilon}^e + \underline{\varepsilon}^p$$

- Resolved shear stress, computed by means of the *orientation tensor*, ***m***

$$\tau^s = \underline{\sigma} : \underline{m}^s \qquad \underline{m}^s = \frac{1}{2}(\vec{l}^{\,s} \otimes \vec{n}^s + \vec{n}^s \otimes \vec{l}^{\,s})$$

- A yield function *f s* is defined on each slip system *s* (here with additive hardening)

$$f^s = \left|\tau^s - x^s\right| - r^s$$

- Viscoplastic flow Shear strain rate s deduced from resolved shear stress s and from the value of the kinematic (Xs) and isotropic (Rs) variables :

$$\dot{\gamma}^s = \left\langle \frac{\left|\tau^s - x^s\right| - r^s}{K^s} \right\rangle^{n^s} sign(\tau^s - x^s)$$

Single crystal model

- Viscoplastic potential [Mandel, 1972]

$$\Omega(\underline{\sigma},\ldots) = \sum_s \frac{K}{n+1}\left\langle \frac{f^s}{K} \right\rangle^{n+1}$$

- Viscoplastic strain rate (from the viscoplastic potential)

$$\dot{\underline{\varepsilon}}^p = \sum_s \frac{\partial \Omega}{\partial \underline{\sigma}} = \sum_s \frac{\partial \Omega}{\partial f^s}\frac{\partial f^s}{\partial \underline{\sigma}} = \sum_s \dot{v}^s \underline{m}^s \eta^s = \sum_s \dot{\gamma}^s \underline{m}^s$$

- Hardening rules : X^s and R^scomputed by means of state variables s and r^s

$$X^s = c\alpha^s \qquad \dot{\alpha}^s = \left(\eta^s - d\alpha^s\right)\dot{v}^s$$

$$R^s = r_0 + Q\sum_j h_{sj} r^j \qquad \dot{r}^j = (1 - br^j)\dot{v}^j$$

Interaction matrix

$$
\begin{array}{cc}
 & \begin{matrix} B4 & B2 & B5 & D4 & D1 & D6 & A2 & A6 & A3 & C5 & C3 & C1 \end{matrix} \\
\begin{matrix} B4 \\ B2 \\ B5 \\ D4 \\ D1 \\ D6 \\ A2 \\ A6 \\ A3 \\ C5 \\ C3 \\ C1 \end{matrix} &
\begin{bmatrix}
h_1 & h_2 & h_2 & h_4 & h_5 & h_5 & h_5 & h_6 & h_3 & h_5 & h_3 & h_6 \\
 & h_1 & h_2 & h_5 & h_3 & h_6 & h_4 & h_5 & h_5 & h_5 & h_6 & h_3 \\
 & & h_1 & h_5 & h_6 & h_3 & h_5 & h_3 & h_6 & h_4 & h_5 & h_5 \\
 & & & h_1 & h_2 & h_2 & h_6 & h_5 & h_3 & h_6 & h_3 & h_5 \\
 & & & & h_1 & h_2 & h_3 & h_5 & h_6 & h_5 & h_5 & h_4 \\
 & & & & & h_1 & h_5 & h_4 & h_5 & h_3 & h_6 & h_5 \\
 & & & & & & h_1 & h_2 & h_2 & h_6 & h_5 & h_3 \\
 & & & & & & & h_1 & h_2 & h_3 & h_5 & h_6 \\
 & & & & & & & & h_1 & h_5 & h_4 & h_5 \\
 & & & & & & & & & h_1 & h_2 & h_2 \\
 & & & & & & & & & & h_1 & h_2 \\
 & & & & & & & & & & & h_1
\end{bmatrix}
\end{array}
$$

simplified version (Taylor model)

$h1 = h2 = h3 = h4 = h5 = h6 = 1$

Example of monocrystal behaviour

Stress–strain curves simulated for a β-titane monocrystal under tension in different directions.

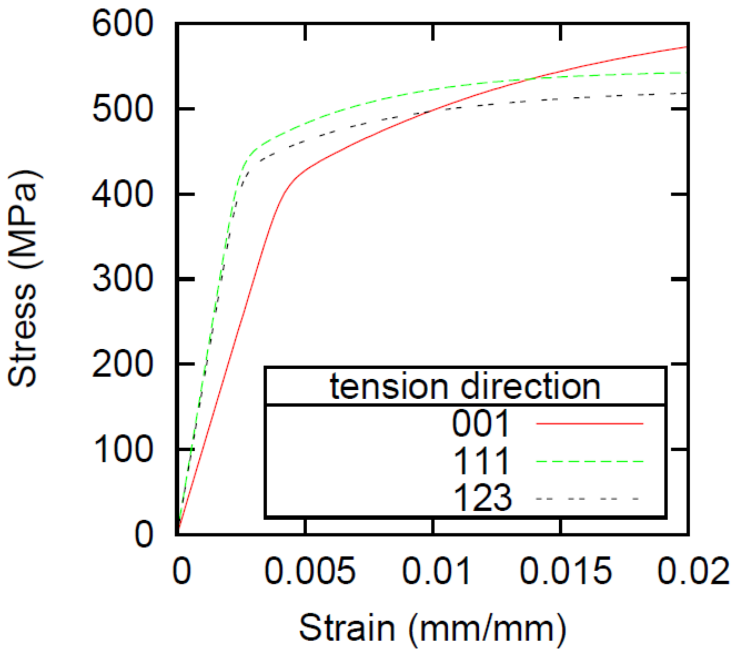

Cubic elasticity

C11 (MPa)	150000
C12 (MPa)	75000
C44 (MPa)	112000

Crystal plasticity

τ_0 (MPa)	Q (MPa)	b	K (Mpa)	n	h_{ij}
100	10	350	500	5	1

Example of monocrystal behaviour

Stress–strain curves simulated for a nickel bas superalloys monocrystal under tension in different directions at 650 °C.

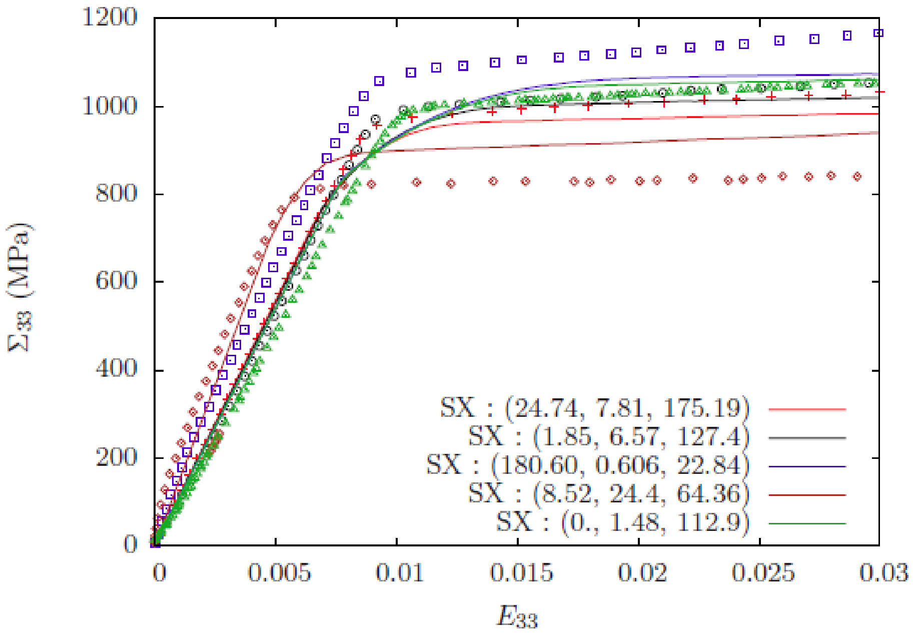

Temperature : 650 °C

$$C_{1111} = 203760 \text{ MPa}$$
$$C_{1122} = 125490 \text{ MPa}$$
$$C_{1212} = 112000 \text{ MPa}$$

« fast » potential

$$n = 11.$$
$$K = 10.3 \text{ MPa.s}^{\frac{1}{n}}$$

$$\tau_c = 337 \text{ MPa}$$
$$c1 = 110\,425 \text{ MPa}$$
$$d1 = 1\,165$$
$$c2 = 504 \text{ MPa}$$

« slow » potential

$$n = 6.5$$
$$K = 2000 \text{ MPa.s}^{\frac{1}{n}}$$

$$\tau_c = 1000 \text{ MPa}$$

Yield surface

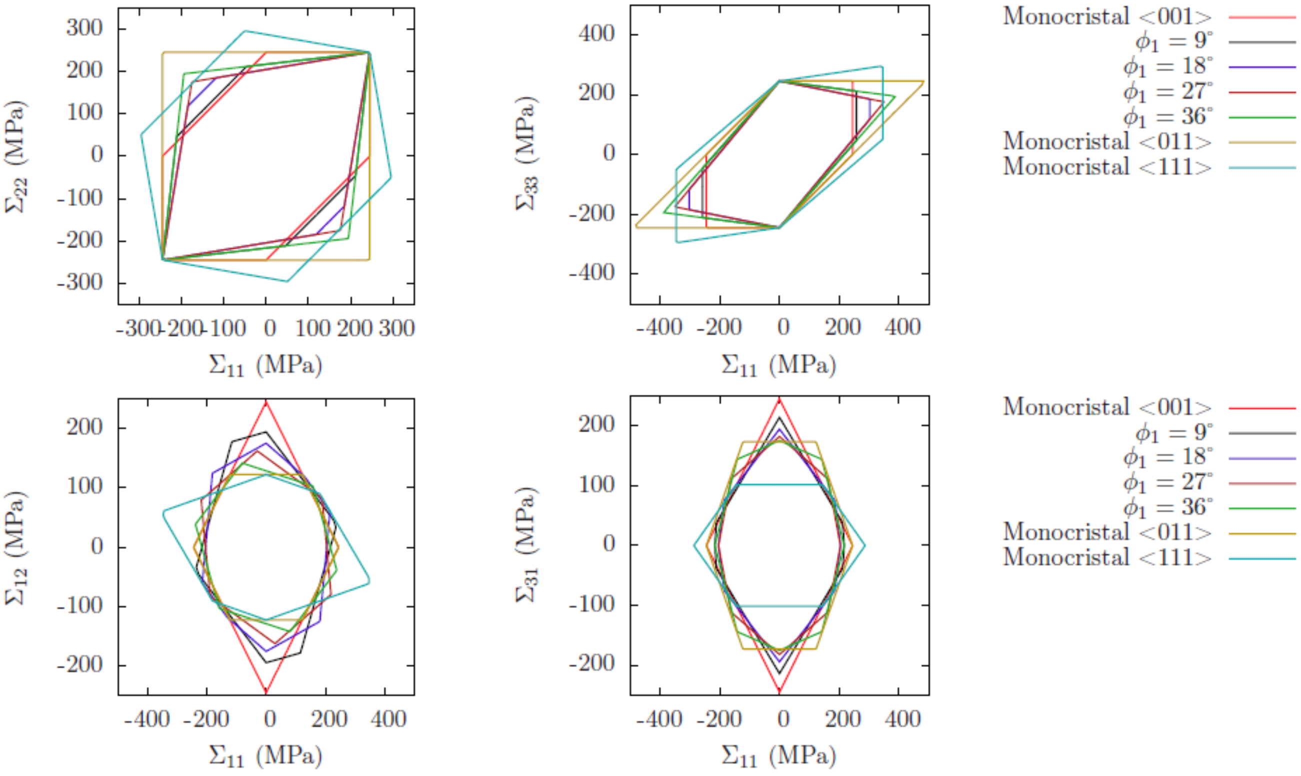

Z-sim input file to compute the yield surface

```
****simulate
 ***test polysurf
  **load
   *segment 1
     time  sig11 sig22 sig33 sig12 sig23 sig31
      0.0  0.    0.    0.    0.    0.    0.
      0.01 0.    1.    0.    0.    0.    0.
  **model
   *file ti.mat
   *rotation euler x1 1. 0. 0. x2 1. 1. 1.
   *integration runge_kutta 1.e-4
  **output
  **yield_surface ps-11-12.test
   *degrees 1.
   *factor 1.e9
   *find_offset 1.e-1
   *component sig11 sig12
   *time 0.0
****return
```

Crack in Ni based superalloy single crystals

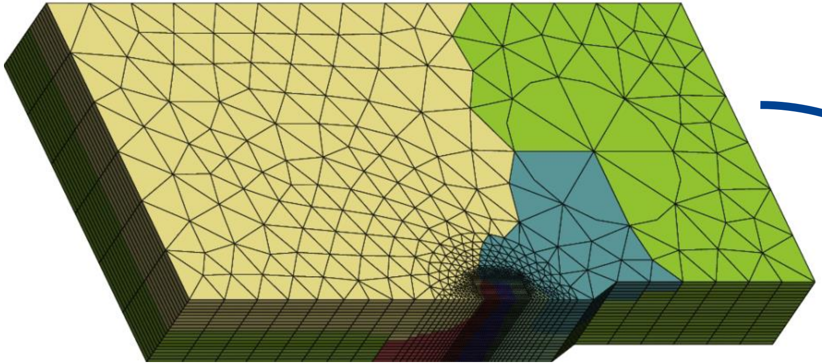

3D mesh of a CT25 specimen

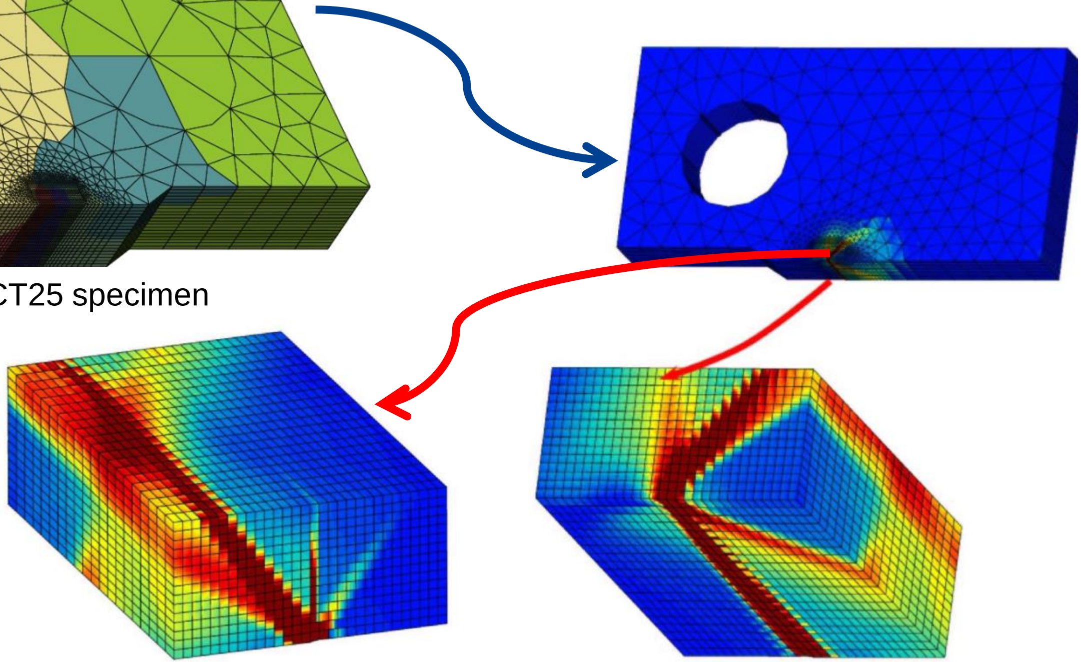

Mid section

Surface

Ph. D. thesis S. Flouriot
Mines ParisTech (2000)

SAFRAN

Crack in Ni based superalloy single crystals

Comparison with experiments [Flouriot et al., 2003]

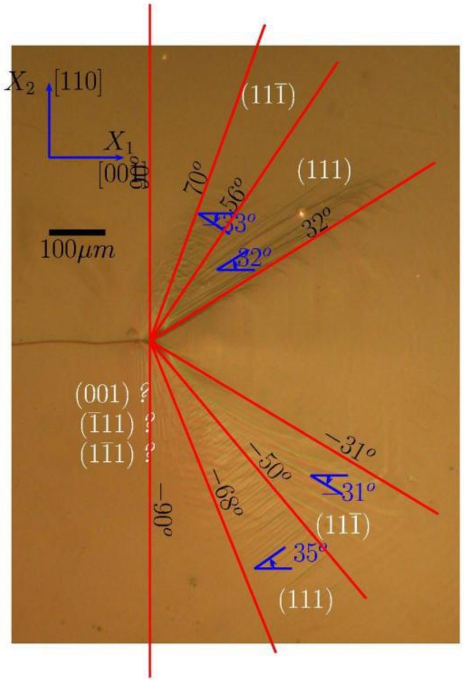

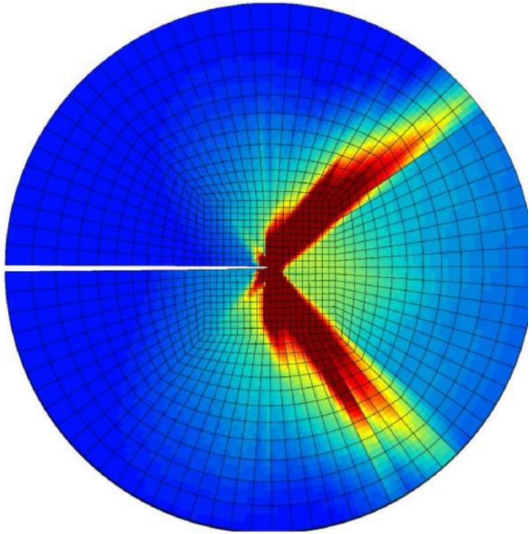

Surface of the specimen
3D F.E. Simulation

Small strain crystal plasticity – AM1

Cubic elasticity $\underline{\sigma} = \underline{\underline{C}} : \underline{\varepsilon}^e$

Resolved shear stress $\tau^s = \underline{\sigma} : \underline{m}^s$

Viscous flow $\dot{\gamma}^s = \varepsilon_0^s \sinh\left(\left\langle \frac{|\tau^s - x^s| - r^s}{K^s} \right\rangle^{n^s}\right) sign(\tau^s - x^s)$

Plastic strain rate $\dot{\underline{\varepsilon}}^p = \sum_s \dot{\gamma}^s \underline{m}^s$

Orientation tensor $\underline{\underline{m}}^s = \frac{1}{2}(\vec{n}^s \otimes \vec{l}^s + \vec{l}^s \otimes \vec{n}^s)$

Kinematic hardening restoration $\dot{x}^s = C^s \dot{\gamma} - D^s x^s |\dot{\gamma}^s| - \left(\frac{|x^s|}{M^s}\right)^{m^s} sign(x^s)$

Small strain crystal plasticity – AM1

saturation of viscosity

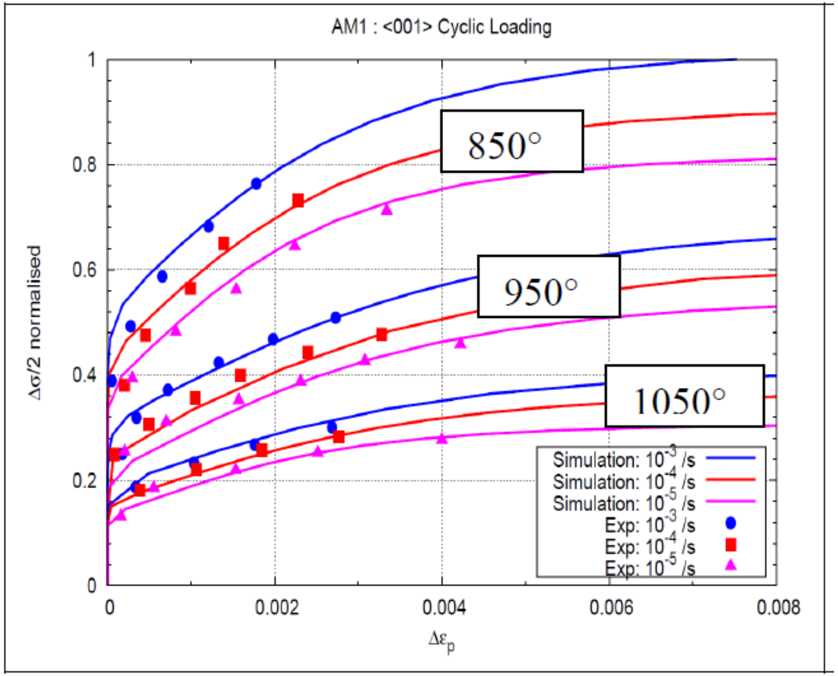

Comparison between simulations and experiments for some isothermal cyclic strain tests.

Use of sinh instead of power law (Norton-Hoff)

Goals : the use of a "sinh" form limits the increase of the viscous stress when the strain rate increases

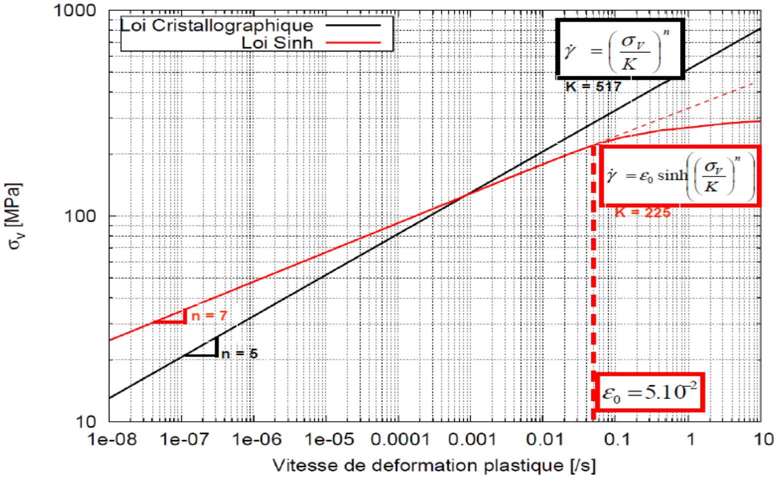

Small strain crystal plasticity – AM1

Concerning creep tests, the introduction of a static recovery term enables to simulate with quite good accuracy the secondary creep

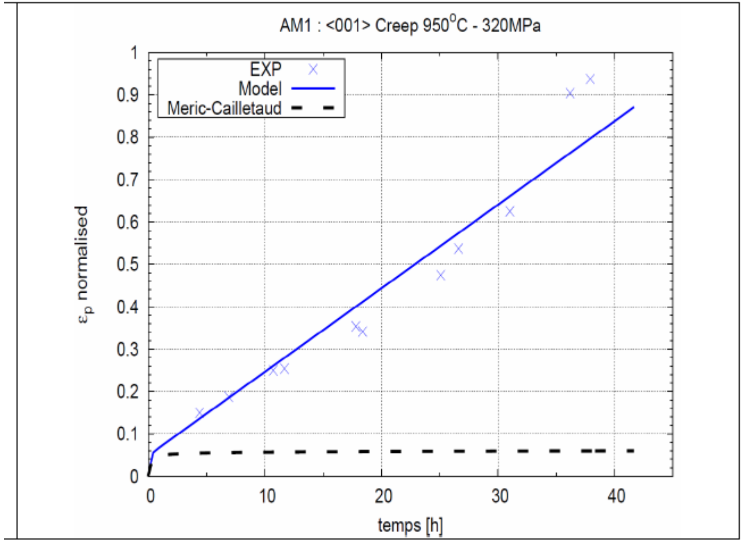

Comparison between simulations and experiments for some creep tests.

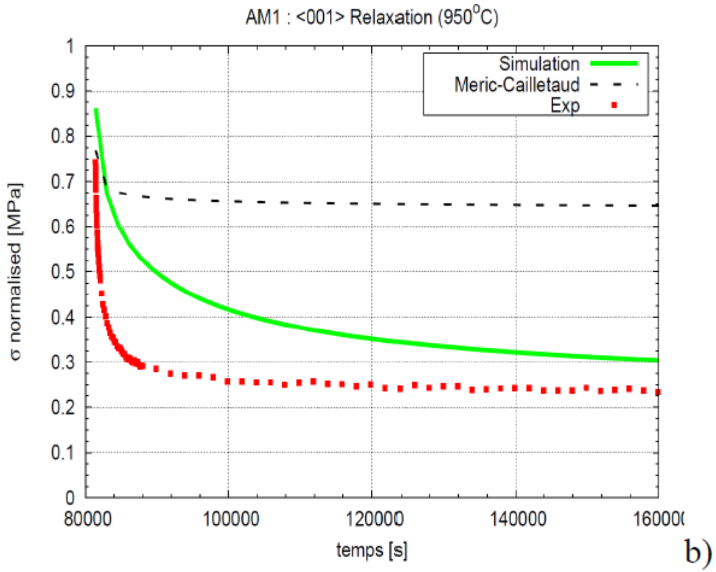

Long term relaxation at 950°C

Small strain crystal plasticity – AM1

Hysteritic loop at 950 °C

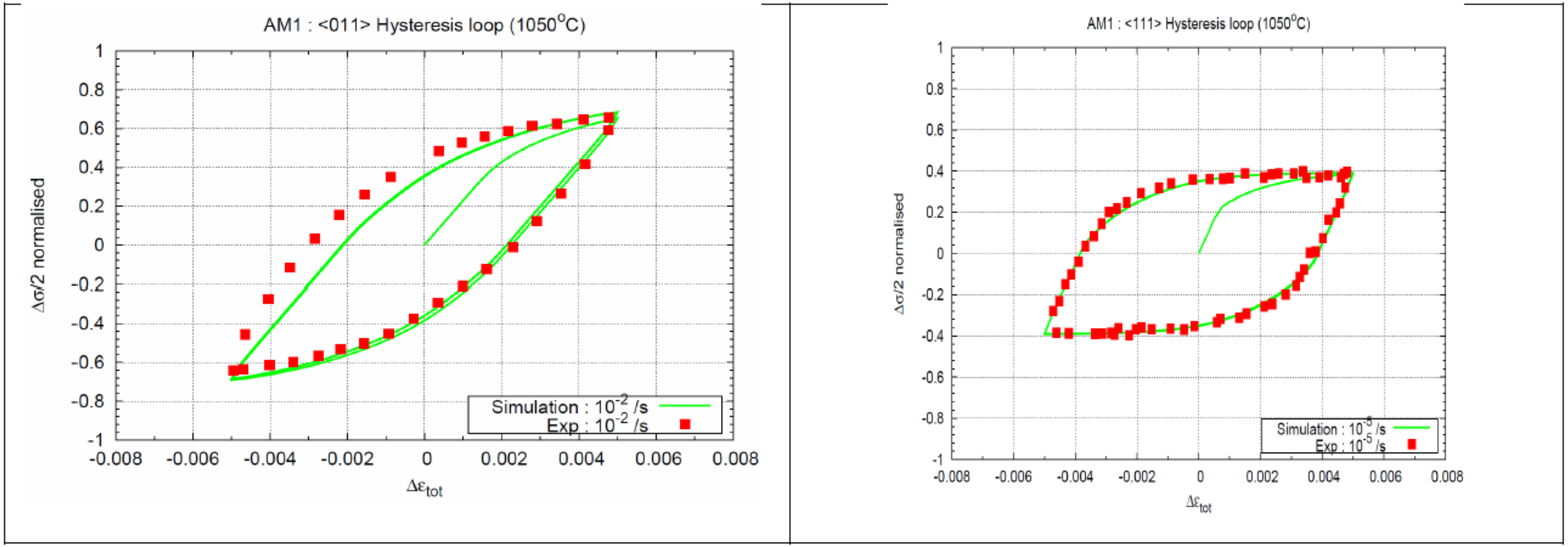

Comparison between simulations and experiments for some hysteresis loops performed along <011> and <111> crystallographic directions

Small strain crystal plasticity – AM1

Simulation of the evolution of the 0,2% yield stress with temperature for three strain rates in the <001> direction

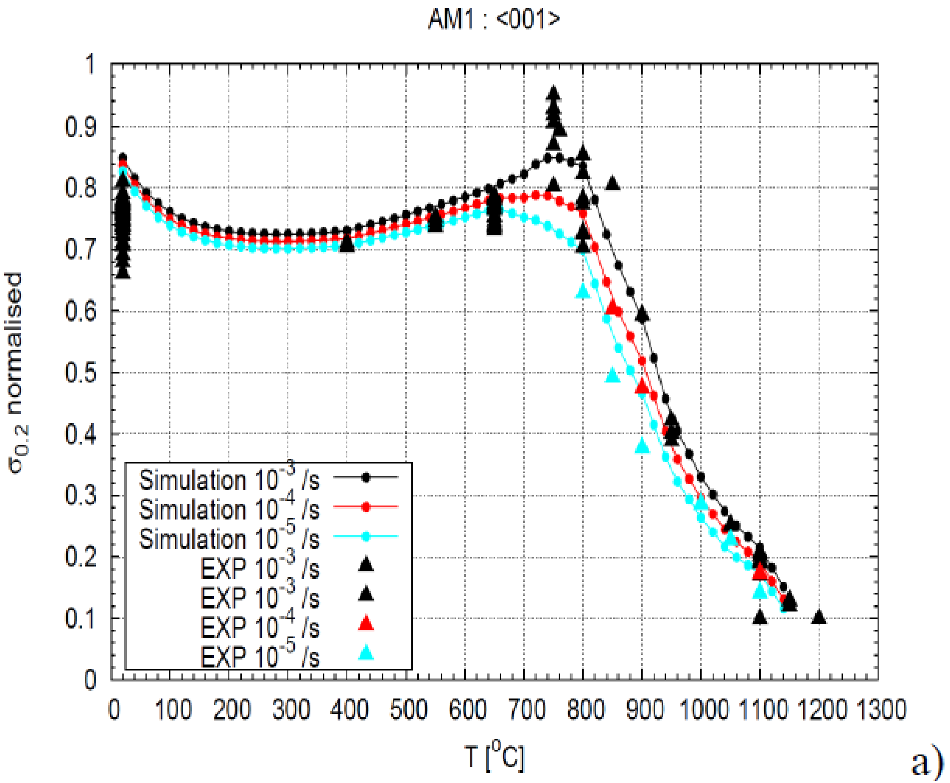

Small strain crystal plasticity – AM1

In a second step, in order to test the material under conditions closer than those observed in service, specific tests were developed called: thermomechanical tests. In such tests, the material is simultaneously subjected to mechanical strain and temperature, both, evolving during the cycle.

Dénomination du cycle	Cyclage en température	Cyclage mécanique
S_1	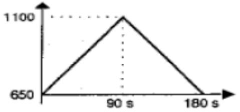 650°C - 1100°C	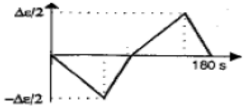 $R_\varepsilon = -1$
S_2	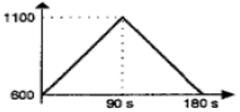 600°C - 11[illegible]	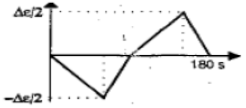 $R_\varepsilon = -1$

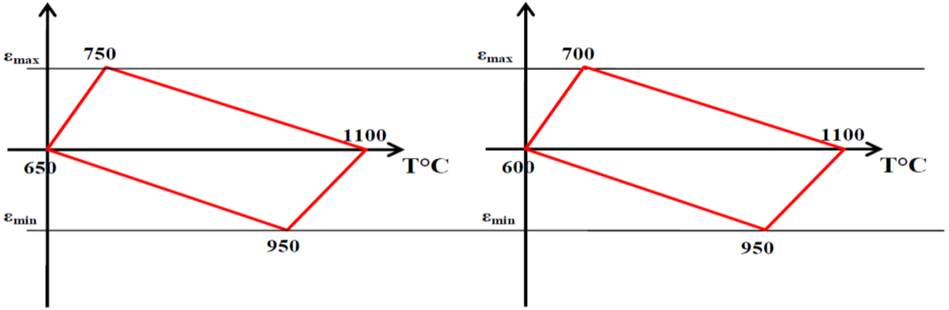

Figure 54.- Évolution de la déformation mécanique en fonction de la température : a) cycle S1, b) cycle S2.

Small strain crystal plasticity – AM1

Comparison between simulations and experiments for some anisothermal test

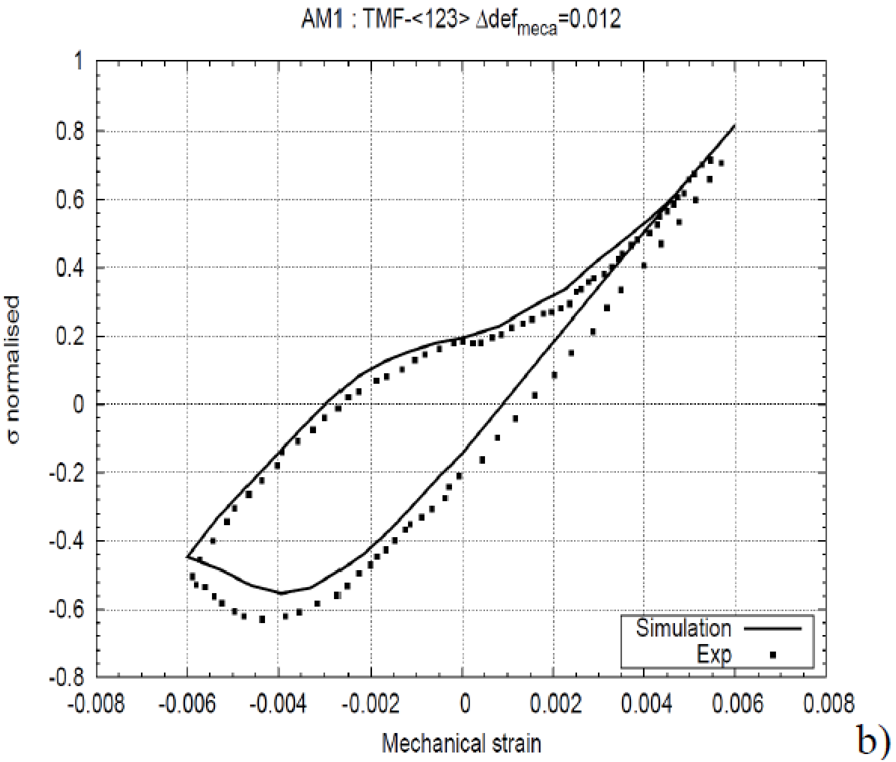

Small strain crystal plasticity – AM1

Synthèse avantage/inconvénient des différents modèles de comportement

	Modèle isotrope à 2 Potentiels de Norton	Modèle anisotrope cristallographique initial à 1 Potentiel de Norton	Modèle « Sinh+restauration »
Anisotrope cristalline	NON	OUI	**OUI**
Prise en compte de la restauration statique de l'écrouissage	NON	NON	**OUI**
Prise en compte du fluage	OUI *mais* ***uniquement*** *dans la direction <001> du monocristal*	NON	**OUI**
Saturation de la viscosité	NON	NON	**OUI**

References

Asaro, R. and Rice, J. (1977).
Strain localization in ductile single crystals.
Journal of the Mechanics and Physics of Solids, 25 :309–338.

Asaro, R. J. (1975).
Elastic-plastic memory and kinematic-type hardening.
Acta Metallurgica, 23 :1255–1265.

Bishop, J. and Hill, R. (1951).
A theoretical derivation of the plastic properties of a polycrystalline face–centered metal.
Philosophical Magasine, 42 :414–427.

Flouriot, S., Forest, S., Cailletaud, G., Koster, A., Remy, L., Burgardt, B., Gros, V., Mosset, S., and Delautre, J. (2003).
Strain localization at the crack tip in single crystal ct specimens under monotonous loading : 3d finite element analyses and application to nickel-base superalloys.
International Journal of Fracture, 124(1-2) :43–77.

References

Hanriot, F., Cailletaud, G., and Remy, L. (1991).
Mechanical behavior of a nickel-base superalloy single crystal.
In *American Society of Mechanical Engineers, Materials Division*, volume 26, pages 139–150

Havner, K. (1992).
Finite Plastic Deformation of Crystalline Solids.
Cambridge University Press.

Hill, R. (1966).
Generalized constitutive relations for incremental deformation of metal crystals by multislip.
JMPS, 14 :95–102.

Hill, R. and Rice, J. (1972).
Constitutive analysis of elastic–plastic crystals at arbitrary strains.
Journal of the Mechanics and Physics of Solids, 20 :401–413.
Kocks, U. (1970).
The relation between polycrystal deformation and single-crystal deformation.
Metallurgical and Materials Transactions, 1(5) :1121–1143.

References

Kocks, U. F. and Brown, T. J. (1966).
Latent hardening in aluminium.
Acta Metallurgica, 14 :87–98.

Mandel, J. (1972).
Plasticité classique et viscoplasticité.
CISM Courses and Lectures No. 97, Udine, Springer Verlag, Berlin.

Meric, L. and Cailletaud, G. (1991).
Single crystal modeling for structural calculations : Part 2—finite element implementation.
Journal of Engineering Materials and Technology, 113(1) :171–182.

Meric, L., Poubanne, P., and Cailletaud, G. (1991).
Single crystal modeling for structural calculations : Part 1—model presentation.
Journal of Engineering Materials and Technology, 113(1) :162–170.

References

Schmid, E. and Boas, W. (1950).
Plasticity of crystals.
Chapman & Hall.

Shan, Z. W., Mishra, R. K., Syed Asif, S. A., Warren, O. L., and Minor, A. M. (2007).
Mechanical annealing and source-limited deformation in submicrometre-diameter Ni crystals.
Nature MAterials, 7(2) :115–119.

Taylor, G. (1938).
Plastic strain in metals.
Journal of the Institute of Metals, 62 :307–324.